Environmental Science and Pollution Research (2021) 28:59329–59344
https://doi.org/10.1007/s11356-020-10943-5

RECENT DEVELOPMENTS AND INNOVATIVE STRATEGIES IN ENVIRONMENTAL SCIENCES IN EUROPE

Composition analysis of $PM_{2.5}$ at multiple sites in Zhengzhou, China: implications for characterization and source apportionment at different pollution levels

Xiaohan Liu[1] · Nan Jiang[2] · Ruiqin Zhang[2] · Xue Yu[1] · Shengli Li[2] · Qingqing Miao[1]

Received: 26 April 2020 / Accepted: 20 September 2020 / Published online: 2 October 2020

Abstract

Zhengzhou is one of the most heavily polluted cities in China. This study collected samples of $PM_{2.5}$ (atmospheric fine particulate matter with aerodynamic diameter ≤ 2.5 μm) at five sites in different functional areas of Zhengzhou in 2016 to investigate the chemical properties and sources of $PM_{2.5}$ at three pollution levels, i.e., $PM_{2.5} \leq 75$ μg/m^3 (non-pollution, NP), 75 μg/m^3 < $PM_{2.5}$ ≤ 150 μg/m^3 (moderate pollution, MP), and $PM_{2.5} > 150$ μg/m^3 (heavy pollution, HP). Chemical analysis was conducted, and source categories and potential source region were identified for $PM_{2.5}$ at different pollution levels. The health risks of toxic elements were evaluated. Results showed that the average $PM_{2.5}$ concentration in Zhengzhou was 119 μg/m^3, and the sum of the concentrations of SO_4^{2-}, NO_3^-, and NH_4^+ increased with the aggravation of pollution level (23, 42, and 114 μg/m^3 at NP, MP, and HP days, respectively). Positive Matrix Factorization analysis indicated that secondary aerosols, coal combustion, vehicle traffic, industrial processes, biomass burning, and dust were the main sources of $PM_{2.5}$ at three pollution levels, and accounted for 38.4%, 21.6%, 16.7%, 7.4%, 7.7%, and 8.1% on HP days, respectively. Trajectory clustering analysis showed that close-range transport was one of the dominant factors on HP days in Zhengzhou. The potential source areas were mainly located in Xinxiang, Kaifeng, Xuchang, and Pingdingshan. Significant risks existed in the non-carcinogenic risk of As (1.4–2.3) for children at three pollution levels and the non-carcinogenic risk of Pb (1.0–1.4) for children with NP and MP days.

Keywords Fine particle · Pollution characteristics · Positive Matrix Factorization · Hybrid Single-Particle Lagrangian Integrated Trajectory Model · Enrichment factor · Health risk assessment

Responsible Editor: Gerhard Lammel

Highlights
- The mean levels of $PM_{2.5}$ on NP, MP, and HP days were 52, 107, and 253 μg/m^3.
- OC/EC ratios of 8.2, 7.6, and 9.8 were recorded on NP, MP, and HP days.
- The SAs had the highest contributions during every pollution levels.
- Significant non-carcinogenic risk of As and Pb exists for children.
- Risks of toxic elements on HP days were greater than those on the other days.

Electronic supplementary material The online version of this article (https://doi.org/10.1007/s11356-020-10943-5) contains supplementary material, which is available to authorized users.

✉ Nan Jiang
jiangn@zzu.edu.cn

[1] College of Chemistry, Zhengzhou University, Zhengzhou 450001, China

[2] School of Ecology and Environment, Zhengzhou University, Zhengzhou 450001, China

Introduction

Due to rapid economic development, successful urbanization, and excessive energy consumption, regional air pollution, especially fine particle ($PM_{2.5}$) pollution, have been identified as the most serious environmental problem in China and considered one of the major concerns of the government, scientists, and the public (Tan et al. 2009; Zhang et al. 2015a). $PM_{2.5}$ pollution mainly occurs in the developed and large population of urban agglomerations, and the most polluted areas include the Yangtze River Delta (Fu et al. 2008), Beijing–Tianjin–Hebei (Zhao et al. 2009), Pearl River Delta (Tao et al. 2014), and Central Plains Economic Region (CPER; Jiang et al. 2017).

$PM_{2.5}$ pollution has a profound impact on the ecosystem, visibility, traffic safety, economy, and interaction with climate (Chow et al. 2002; Andreae and Rosenfeld 2008; Zhang et al. 2015a). $PM_{2.5}$ contains various toxic substances that negatively affect human health (Coyle et al. 2006; Cakmak et al.

2014). These chemical components are mainly derived from various human factors, such as coal combustion, automobile emissions, building dust re-suspension, biomass combustion, and industrial-related emissions. Controlling these pollution sources is the key to reducing $PM_{2.5}$ concentrations and enhancing air quality.

For $PM_{2.5}$ source apportionment, a multivariate analysis technique, namely, Positive Matrix Factorization (PMF), which was developed by Paatero and Tapper (1994), has been applied to conduct source analysis (Ogulei et al. 2005; Gildemeister et al. 2007; Subramanian et al. 2007; Liu et al. 2019). Backward trajectory and potential source contribution function (PSCF) models have been used to determine the transport pathways of air masses and the potential source regions of pollutants at sampling sites, respectively (Liu et al. 2018).

Zhengzhou is the core city of the CPER, with a high density of coal consumption and dense transportation systems and industries. In 2016, 30.8 Mt of coal was used by industrial enterprises whose main business income exceeded 20 million Yuan (1 USD ≅ 6.95 Yuan in 2016), and various transport modes (railway, highway, and civil aviation) completed the freight of 220.4 Mt and the passenger traffic of 163.6 million persons (Bureau of Statistics of Zhengzhou 2017). Zhengzhou is surrounded by Xinxiang, Jiaozuo, Luoyang, Kaifeng, and Xuchang and near Hebei, Shandong, Anhui, Hubei, Shaanxi, and Shanxi Provinces, which are all densely populated and industrialized cities; these areas are frequently reported to have serious air pollution because of the dense emission of air pollutants (Wang et al. 2014, 2020a, b; Wang 2016; Liang et al. 2016; Feng et al. 2018; Jiang et al. 2019). With the intensive pollutant emission and adverse meteorological conditions in Zhengzhou, heavy $PM_{2.5}$ load and low visibility occur frequently. Jiang et al. (2018a) showed that the average $PM_{2.5}$ concentration in Zhengzhou dropped from 191 μg/m^3 in 2013 to 150 μg/m^3 in 2015. Although the annual mean concentration has decreased because of efforts from the local government, pollution remains serious and much higher than the annual limit of $PM_{2.5}$ (35 μg/m^3) in the Chinese National Ambient Air Quality Standard (NAAQS), especially in winter in 2015 when the average $PM_{2.5}$ concentration reached 191 μg/m^3 with the frequent occurrence of heavy pollution. Therefore, a comprehensive research on different $PM_{2.5}$ levels is a key factor of environmental management transition (i.e., from extensive management to refine management) in Zhengzhou. Huang et al. (2017) conducted a hierarchical study of $PM_{2.5}$ in the Beijing–Tianjin–Hebei region, indicating that $PM_{2.5}$ components and source contributions were different in different pollution levels. There have been several reports on the study of $PM_{2.5}$ chemical components and source analysis at one sampling site in Zhengzhou (Wang et al. 2015; Jiang et al. 2018a, b; Li et al. 2019). However, these results only represent the pollution level around a particular sampling site, not the pollution situation of Zhengzhou city as a whole. Only two studies have focused on the temporal and spatial distribution and source of $PM_{2.5-bound}$ elemental components at multiple sampling sites in Zhengzhou (Jiang et al. 2019; Liu et al. 2019). However, all the components in the spatial and temporal distribution and sources of $PM_{2.5}$ at different $PM_{2.5}$ levels at multiple sites in Zhengzhou have yet to be explored.

In this study, five sampling sites were set up in Zhengzhou to simultaneously collect $PM_{2.5}$ samples. Their chemical compositions were analyzed, and source distributions of $PM_{2.5}$ at different pollution levels were determined by PMF model. In this study, daily $PM_{2.5}$ < 75 μg/m^3, 75 μg/m^3 ≤ daily $PM_{2.5}$ < 150 μg/m^3, and daily $PM_{2.5}$ ≥ 150 μg/m^3 were defined as non-pollution (NP) days, moderate pollution (MP) days, and heavy pollution (HP) days, respectively (Ministry of Environmental Protection of the People's Republic of China 2012). Hybrid Single-Particle Lagrangian Integrated Trajectory (HYSPLIT) and PSCF models were employed to analyze the potential region of $PM_{2.5}$ concentration and sources in Zhengzhou. This study could help comprehensively elucidate $PM_{2.5}$ at different pollution levels in cities with a similar contamination status and provide technical support for relevant government departments to formulate policies, especially for the control measures with relatively large contribution of pollution sources in HP days.

Materials and methods

Sampling

In this study, $PM_{2.5}$ samples were collected synchronously at five sites, including traffic, industrial, and scenic sites, in each season from February to December of 2016. The detailed description and distribution of the site are shown in Table S1 and Fig. 1.

A total of 542 samples, including 271 samples for quartz microfiber filters (90 mm in diameter, PALLLFLEX, USA) and 271 samples for polypropylene filters (90 mm in diameter, Tianjin Xinyao, China), were collected from 10:00 AM on a previous day to 9:00 AM on the next day by using middle-volume samplers (100 L/min; TH-150AII, Tianhong, China) on the roof of buildings at the five sites. More detailed descriptions can be found in the Supplemental Materials and our previous study (Jiang et al. 2018a; Liu et al. 2019).

Sample analysis

Chemical composition analysis

The concentrations of organic carbon (OC) and elemental carbon (EC) were analyzed using a carbon analyzer (Sunset Laboratory, USA). More details of process can be found in Supplemental Materials and Jiang et al. (2018c). Water-soluble inorganic ions

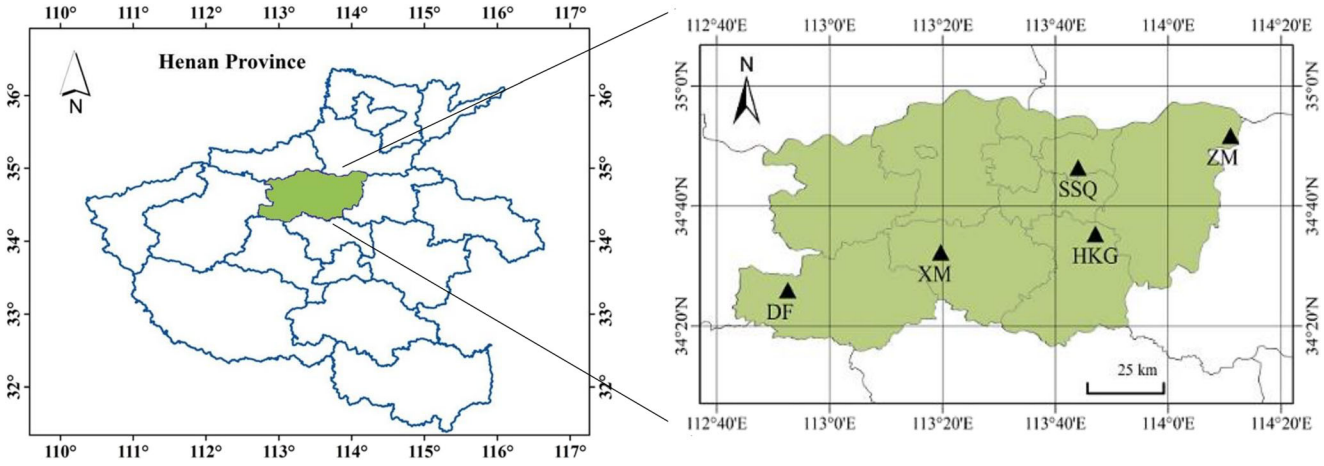

Fig. 1 Locations of sampling sites in Zhengzhou

(WSIIs, i.e., F^-, Cl^-, NO_3^-, SO_4^{2-}, Na^+, NH_4^+, K^+, Mg^{2+}, and Ca^{2+}) were measured through ion chromatography (ICS-900, ICS-90, Dionex, USA). Further information was described in Supplemental Materials and our previous study (Jiang et al. 2018a). Twenty inorganic elements, including Na, Mg, Al, and Si, in the samples were analyzed using an S8 TIGER wavelength scattering X-ray fluorescence spectrometer (Bruker, Germany). For more details, see Supplemental Materials and our previous study (Jiang et al. 2019).

Chemical mass closure

Chemically reconstructed $PM_{2.5}$ mass was calculated as the sum of the compounds, including organic matter (OM), EC, NH_4^+, NO_3^-, Cl^-, SO_4^{2-}, crust elements, and trace elements. OM was estimated by multiplying OC by 1.8 (Chow et al. 1996; Simon et al. 2011).

The crust elements were calculated as follows (Tian et al. 2016):

$$[\text{Crust elements}]=2.20\times[\text{Al}]+2.42\times[\text{Fe}]+1.63\times[\text{Ca}]+2.49\times[\text{Si}]+1.94\times[\text{Ti}] \quad (1)$$

Trace element content referred to the sum of 14 different element species and could be expressed as follows:

$$[\text{Trace elements}]=\text{Ni}+\text{Na}+\text{Pb}+\text{Mg}+K+\text{Cr}+V+\text{Cu}+\text{Zn}+\text{Ba}+\text{Sb}+\text{Mn}+\text{As}+\text{Se} \quad (2)$$

PMF model

Input data included the concentrations and uncertainties for all species. Species concentration data, missing data, and lower method detection limit value pretreatment and uncertainty determination were conducted in accordance with the PMF 5.0 User Guide (U.S. EPA 2014). Species classification was determined using the signal-to-noise ratio (S/N). When $S/N > 1$, $0.5 < S/N < 1$, and $S/N < 0.5$, the species was marked as "strong," "weak," and "bad," respectively. Moreover, if certain species are poorly modeled, they should be classified as "bad" based on the observed versus predicted scatter plots and time series. Bootstrap (BS) and displacement were used to estimate random error in matrix and rotational ambiguity, respectively (Paatero et al. 2014). BS was run with 100 resamples, and in PMF analysis mapping, it is acceptable for all PM factors to account for more than 80% of BS runs. Fpeak is a function that estimates the lower limit of rotational uncertainty (Reff et al. 2007; Manousakas et al. 2017). In our study, Fpeak varied from − 2 to + 2 to determine Q/Q_{exp}.

Back trajectory cluster

Considering that the SSQ site is a national environmental air quality monitoring station, the online data is complete and the data quality can be guaranteed, and the site is located in the city center, this study selected SSQ site for backward trajectory analysis and to represent the regional transmission influence of Zhengzhou. In this study, 48 h air mass backward trajectories arriving in Zhengzhou (height: 100 m) were calculated at three pollution levels. The model was run 4 times a day at 0:00, 06:00, 12:00, and 18:00 UTC. Cluster analysis was then performed using the HYSPLIT model.

PSCF model

In this study, the PSCF model was used to identify the potential source areas of $PM_{2.5}$ and their sources at SSQ site driven by meteorological fields. The domain of PSCF was 26.94°–59.04° N and 66.20°–122.24° E with a horizontal resolution of 0.3° × 0.3°. Other detailed descriptions can be found in our previous study (Jiang et al. 2019).

Health risk assessment

In this study, the health risk assessment model developed by the US Environmental Protection Agency was used to assess the carcinogenic risk of As, Pb, and Ni and the non-carcinogenic risk of V, Cu, As, Mn, Zn, Pb, and Ni. The target subjects were classified as children and adults and exposure routes were divided into ingestion, inhalation, and dermal. Exposure and risk assessment method was referred to US EPA (1989, 2004, 2009). As the average life expectancy and weight of Chinese and foreigners were different, the parameters of lifetime and body weight of Chinese were adopted in this study, and other relevant parameters were from the official website of US EPA. And the selection of parametric exposure frequency was based on the number of days corresponding to different pollution levels in this study. Other detailed descriptions can be found in the Supplemental Materials.

The non-carcinogenic risk index hazard quotient (HQ), hazard index (HI, HQ sum), and carcinogenic risk index (CR) of the elements were calculated as follows:

$$CR_{inhale} = IUR \times EC_{inhale} \quad (3)$$

$$CR_{ingest} = CDI_{ingest} \times SF_O \quad (4)$$

$$CR_{dermal} = DAD_{dermal} \times \frac{SF_O}{GIABS} \quad (5)$$

$$HQ_{inhale} = \frac{EC_{inhale}}{(RfC_i \times 1000\mu g/mg)} \quad (6)$$

$$HQ_{ingest} = \frac{CDI_{ingest}}{RfD_O} \quad (7)$$

$$HQ_{dermal} = \frac{DAD_{dermal}}{RfD_O \times} GIABS \quad (8)$$

$$HI \text{ or } CR = \sum_{i=1}^{n} HQ_i \text{ or } CR_i \quad (9)$$

where IUR is the inhalation unit risk $(\mu g/m^3)^{-1}$; EC_{inhale} is the exposure concentration ($\mu g/m^3$); CDI_{ingest} is the chemical daily intake (mg/(kg day)); SF_O is the slope factor $(mg/(kg\ day))^{-1}$; DAD_{dermal} is the dermal absorption dose (mg/(kg day)); GIABS is the gastrointestinal absorption factor; RfC_i is the inhalation reference concentrations, mg/m^3; RfDo is the oral reference dose, mg/(kg day) (US EPA 2011a, b); and HQ_i and CR_i are the risk values of element *i* in the risk assessment model calculation.

Result and discussion

$PM_{2.5}$ concentration level

The time variability of $PM_{2.5}$ concentrations at the five sites (i.e., HKG, ZM, XM, SSQ, and DF) during the sampling period is shown in Fig. S1. The daily changes in $PM_{2.5}$ concentrations indicated that the time-related changes in $PM_{2.5}$ concentrations at the five sampling sites were similar. HP days mainly occurred in winter, while NP days mainly occurred in summer. This condition might be related to the increased anthropogenic emissions in winter (e.g., extra coal-fired heating in northern China) and the effects of meteorological conditions (Fig. S2; e.g., low wind speed, low planetary boundary layer height, and high atmospheric stability) (Han et al. 2015). $PM_{2.5}$ concentrations in summer are low because a strong radiation intensity, a high temperature, a strong airflow, and a high air mixing layer height (Tang et al. 2016) are conducive to the dilution and diffusion of air pollutants, resulting in the lowest $PM_{2.5}$ concentration measurement.

The annual mean $PM_{2.5}$ concentration in average of five sites was 119 ± 98 $\mu g/m^3$ (Table 1), which greatly exceeded the annual concentration standard (35 $\mu g/m^3$) of the Chinese NAAQS. Compared with other cities in China, the annual $PM_{2.5}$ concentration in Zhengzhou was higher than that in Shanghai (83 $\mu g/m^3$; Wang et al. 2016), Xi'an (108 $\mu g/m^3$; Dai et al. 2018), Heze (1001 $\mu g/m^3$; Liu et al. 2017), Beijing (85 $\mu g/m^3$), Tianjin (87 $\mu g/m^3$), Tangshan (100 $\mu g/m^3$), Chengdu (54 $\mu g/m^3$), Langfang (90 $\mu g/m^3$) (Chen et al. 2017), and Guangzhou (75 $\mu g/m^3$; Liu et al. 2014), indicating a very serious $PM_{2.5}$ pollution. Throughout the sampling period, the proportions of sample quantities on NP, MP, and HP days were 40%, 37%, and 23%, and the $PM_{2.5}$ concentrations were 52, 107, and 253 $\mu g/m^3$, respectively. This shows that $PM_{2.5}$ contributes the most in HP days. In addition, the highest total number of MP and HP days of $PM_{2.5}$ at the five sampling sites was recorded in the SSQ site (76%), and this may be the SSQ site was located in the city center with dense population and large traffic flow, and construction near the sampling site, leading to large pollutant emissions. Moreover, the meteorological conditions were more stable in the polluted days, which was conducive to the accumulation of pollutants and leads to the aggravation of pollution.

Chemical composition of $PM_{2.5}$

Carbon components

Table 2 shows that the annual average concentration of total carbonaceous (TC; OC plus EC) was 18 $\mu g/m^3$, accounting for 15% of $PM_{2.5}$. In addition, TC concentration in $PM_{2.5}$ increased from 7.3 $\mu g/m^3$ on NP days to 15 $\mu g/m^3$ on MP days and 39 $\mu g/m^3$ on HP days. The proportion of TC on HP days was 16%, which was higher than that on NP days (14%) and MP days (14%). This was related to the increase of pollutants emitted from fossil fuel combustion in HP days, and the inverse stable layer was stronger and thicker, and the increase of static stable weather, which was not conducive to the diffusion of pollutants. Moreover, low temperature is

Table 1 Level of $PM_{2.5}$ concentration (μg/m^3) and the sample numbers (n) and proportion (%) of different pollution days during study period at five sites

Pollution levels	All sites			HKG			ZM			XM			SSQ			DF		
	μg/m^3	n	%	μg/m^3	n	%	μg/m^3	n	%	μg/m^3	n	%	μg/m^3	n	%	μg/m^3	n	%
NP	52 ± 15	108	40	55 ± 12	15	30	48 ± 12	29	53	50 ± 21	24	42	57 ± 15	14	24	55 ± 12	26	51
MP	107 ± 22	100	37	107 ± 22	19	38	99 ± 21	12	22	106 ± 24	22	39	107 ± 22	28	48	113 ± 23	19	37
HP	253 ± 121	63	23	230 ± 97	16	32	262 ± 139	14	25	247 ± 88	11	19	258 ± 155	16	28	290 ± 101	6	12
AVE	119 ± 98	271	100	131 ± 91	50	100	114 ± 114	55	100	110 ± 84	57	100	137 ± 113	58	100	104 ± 82	51	100

favorable for semi-volatile matter (e.g., polycyclic aromatic hydrocarbons) to remain in the particulate phase (Li et al. 2019), so that the concentration of TC in the particles was higher in HP days.

EC has good chemical stability because of the incomplete combustion of carbonaceous fuel, and it is often used as a tracer of primary emission sources (Turpin and Huntzicker 1995). OC was derived from both primary particulate matter emitted from fuel combustion and secondary organic carbon (SOC) generated from gaseous organic matter through various photochemical transformations. In this study, the mean OC/EC ratios were 8.2, 7.6, and 9.8 on NP, MP, and HP days, respectively (Table 2). Similar variations were also observed at different pollution levels at the five sites (Table S2). The OC/EC ratios reported in various studies have different emission sources in different ranges, including 1.0–4.2 for vehicle exhaust (Schauer et al. 2002), 3.8–13.2 for biomass burning (Zhang et al. 2007), and 2.5–10.5 for coal combustion (Chen et al. 2006). The main sources of OC and EC emissions at DF site was coal emissions, while the other four sites were coal emissions and biomass combustion.

OC includes primary organic carbon (POC) and SOC. At present, there is no technology that can strictly separate POC and SOC. The minimum OC/EC ratio method for the content of SOC is used for quantitative (Turpin and Huntzicker 1995)

$$\mathrm{SOC} = \mathrm{OC} - \mathrm{POC} = \mathrm{OC} - \left(\frac{\mathrm{OC}}{\mathrm{EC}}\right)_{\min} \quad (10)$$

Table 2 Concentrations of OC (μg/m^3) and EC (μg/m^3) in $PM_{2.5}$ and the OC/EC mass ratio in different pollution levels during the entire sampling period average of all five sites

	All sites				
	OC	EC	OC/EC	TC	SOC
NP	6.5 ± 2.4	0.9 ± 0.4	8.2 ± 3.1	7.3 ± 2.6	2.5 ± 1.9
MP	13 ± 4.5	1.9 ± 0.9	7.6 ± 3.3	15 ± 5.1	5.1 ± 3.2
HP	35 ± 17	4.5 ± 2.7	9.8 ± 7.0	39 ± 18	16 ± 16
AVE	15 ± 14	2.1 ± 2.0	8.3 ± 4.4	18 ± 15	6.5 ± 9.4

where SOC (μg/m^3), EC (μg/m^3), and OC (μg/m^3) are the concentrations of SOC, EC, and OC, respectively, and $(OC/EC)_{min}$ represents the minimum OC/EC ratio in each site across different seasons throughout the sampling period. The results showed that the mean concentration of SOC was 6.5 μg/m^3, and the concentrations of NP, MP, and HP days in Zhengzhou were 2.5, 5.1, and 16 μg/m^3, respectively. Similar variations were also observed at different pollution levels at the five sites (Table S2). The higher concentration of SOC in HP days may be related to the rapid conversion of organic carbon precursors, that is, the rapid conversion of organic carbon precursors, VOCs (Cao et al. 2005).

WSIIs

Table 3 shows that WSIIs accounted for the largest proportion of $PM_{2.5}$ (50%) in Zhengzhou. Secondary inorganic aerosols (SIAs) (SO_4^{2-}, NO_3^-, and NH_4^+) were the most important components in WSIIs, accounting for 88.4%. Ca^{2+}, Cl^-, K^+, Na^+, Mg^{2+}, and F^- had low proportion in WSIIs, and their total proportion in WSIIs was less than 13.0%. The concentrations (μg/m^3) of Ca^{2+}, Cl^-, K^+, Na^+, Mg^{2+}, and F^- decreased in the following order: Cl^- (2.6) > Ca^{2+} (1.5) > K^+ (1.4) > Na^+ (0.4) > F^- (0.2) > Mg^{2+} (0.1) in average of five sites. Additionally, concentrations of all WSIIs were the highest on HP day, whereas the lowest concentrations were recorded on NP days. This may be because HP days occur more often in winter, coal heating leading to an increase in SO_4^{2-} and Cl^- emissions, and burning firewood for heating in some rural areas leading to an increase in K^+ emissions in this season. In addition, due to the combined action of photochemistry and heterogeneous reaction, NOx emission and gas-aerosol balance, the concentration of NO_3^- was larger (Zhang et al. 2013), and the dispersity was poor because of the stability of atmospheric structure in winter, resulting in high pollution levels of WSIIs. NP days occur more often in summer, when the radiation intensity, temperature, airflow, and boundary layer height were strong and conducive to the dilution and diffusion of air pollutants (Tang et al. 2016), resulting in low concentrations of all WSIIs.

Table 3 Concentrations of WSIIs (μg/m^3) in $PM_{2.5}$, SOR, NOR, and WSIIs/$PM_{2.5}$ (%) in different pollution levels during the entire sampling period at all sites in Zhengzhou

	All sites			
	NP	MP	HP	AVE
Na^+	0.2 ± 0.1	0.4 ± 0.3	0.7 ± 0.4	0.4 ± 0.3
NH_4^+	7.0 ± 2.9	11 ± 4.7	27 ± 16	13 ± 11
K^+	0.4 ± 0.2	1.0 ± 0.6	3.6 ± 3.1	1.4 ± 2.0
Mg^{2+}	0.1 ± 0.0	0.1 ± 0.1	0.1 ± 0.1	0.1 ± 0.1
Ca^{2+}	0.8 ± 0.8	1.9 ± 1.3	1.9 ± 2.2	1.5 ± 1.5
F^-	0.1 ± 0.1	0.2 ± 0.2	0.4 ± 0.3	0.2 ± 0.2
Cl^-	0.6 ± 0.6	1.8 ± 1.4	7.3 ± 4.2	2.6 ± 3.5
NO_3^-	6.4 ± 4.4	17 ± 8.7	50 ± 34	20 ± 24
SO_4^{2-}	9.8 ± 3.7	14 ± 5.2	37 ± 28	17 ± 18
SNA	23 ± 9.2	42 ± 17	114 ± 76	51 ± 52
SNA/WSIIs	91 ± 6.2	87 ± 8.4	87 ± 7.8	88 ± 7.7
WSIIs/$PM_{2.5}$	49 ± 13.8	45 ± 15.8	49 ± 13.7	48 ± 14.6
SOR	0.3 ± 0.2	0.4 ± 0.2	0.5 ± 0.2	0.4 ± 0.2
NOR	0.1 ± 0.1	0.3 ± 0.1	0.4 ± 0.2	0.2 ± 0.2

Nitrogen oxidation ratio (NOR = (n NO_3^-)/n NO_3^- + n NO_2, where n NO_3^- and n NO_2 represent the molar concentrations of NO_3^- and NO_2) and sulfur oxidation ratio (SOR = (n SO_4^{2-})/n SO_4^{2-} + n SO_2, where n SO_4^{2-} and n SO_2 represent the molar concentrations of SO_4^{2-} and SO_2) are usually used to indicate the secondary formation degree of nitrate and sulfate (Zhao et al. 2013; Huang et al. 2016). At higher NOR and SOR, more NO_2 and SO_2 in gaseous states are transformed to nitrate and sulfate in the atmosphere. In this study, SOR and NOR increased significantly when $PM_{2.5}$ concentration increased and maintained a high level on HP days (SOR mean 0.5, NOR mean 0.4). Similar variations were also observed on different pollution level days at the five sites (Table S3). Yang et al. (2015) revealed that the significant increase in SOR and NOR on HP days was mostly related to the strong secondary formation of SIAs. However, the increase in SIAs concentration was still significant on HP days.

Elements

In Table 4, the concentration of total elements accounted for only 11% of $PM_{2.5}$ throughout the sampling period, and the average concentration (ng/m^3) of all elements was 11.1 μg/m^3. The concentrations of elements (ng/m^3) are found to be in the order of Ca (3329) > Si (2103) > K (1413) > Fe (1348) > Cl (1117) > Al (913) > Mg (209) > Zn (162) > Ti (114) > Na (106) > Pb (82) > Mn (56) > Ba (45) > Sb (23) > Cu (22) > As (13) > Cr (7.9) > V (7.9) > Se (7.4) > Ni (3.3). The relative abundance of soil-related elements, such as Ca, Si, Fe, Ti, and Al, accounted for 71% of the total elements. Additionally, the concentration of each element in average of five sites increased gradually from NP days to MP days and then to HP days, but the proportion decreased gradually (Tables 4 and S4). This result indicated that the elements were not the main cause of high $PM_{2.5}$ levels on HP days.

Enrichment factors (EFs) are commonly calculated to identify the origin of elements and evaluate the extent of anthropogenic influences (Yang et al. 2010; Rogula-Kozłowska et al. 2013). If EFs are greater than 10, elements are mostly generated by anthropogenic sources; if EFs are close to 1, elements have a crustal origin (Nolting et al. 1999). In this study, EFs were calculated as described by Chen et al. (1991), and Al was used as the reference element for the crust (Hsu et al. 2016). The EF values of the elements in $PM_{2.5}$ on different pollution days in average of five sites are shown in Fig. 2. The EF values of Zn, Na, Ca, Pb, As, Cu, and Sb exceeded 10 on different pollution days, indicating that the elements came from anthropogenic activities (Lough et al. 2004; Zhang et al. 2015b). The EF values of Al, Si, Mg, Fe, and Ti were close to 1, suggesting the crustal origin of the elements. The EF values of V, Mn, K, and Ba were between 1 and 10, implying that the elements came from anthropogenic and crustal sources (Han et al. 2015). The high EFs of As, Cu, Zn, Pb, Sb, and Na varied from 56 to 7709 on NP, MP, and HP days. This result implied that the elements were primarily released by anthropogenic sources and highly enriched. In addition, most of the elements (Na, Sb, Pb, Zn, Cu, As, Ca, Cr, Mn, K, Ba, Fe, Ti, and Mg) had the highest EFs on HP days. The EFs of elements in $PM_{2.5}$ at the five sampling sites and at different pollution levels during study period are shown in Fig. S3. The EF of Ca was higher than 10 in all sites except in the DF site (7.3–9.9). The EFs of Ba and K were below 10 but higher than 1 in the five sites and were above 10 in DF (32, 20), XM (18, 11), and ZM (35, 23) sites during HP period. The EFs of Cr, Ni, V, and Mn (4.6–16) were close to 10, indicating that these elements possibly came from anthropogenic sources.

Chemical mass closure analysis

The comparison of reconstruction results and gravimetric results is shown in Fig. S4. A significant correlation was observed between reconstruction and gravimetric results (R^2 > 0.96), indicating the strong reliability of the chemical reconstruction method. The relative concentrations and contribution of the major chemical components of $PM_{2.5}$ on different pollution days in Zhengzhou are shown in Figs. 3 and S5. $PM_{2.5}$ in Zhengzhou primarily comprised OM (28 μg/m^3, 23%), SIAs (51 μg/m^3, 43%), and crust elements (13 μg/m^3, 11%), and lower proportions of EC (2.1 μg/m^3, 1.8%), chloride (2.6 μg/m^3, 2.2%), and other trace elements (2.3 μg/m^3, 1.9%). Additionally, the concentration of almost all chemical

Table 4 Concentrations (ng/m^3) of elements in $PM_{2.5}$ in different pollution levels during the entire sampling period at all sites in Zhengzhou

	All sites			
	NP	MP	HP	AVE
Element/$PM_{2.5}$ (%)	10 ± 6.1	13 ± 8.4	7.9 ± 7.5	11 ± 7.5
Na	59 ± 39	128 ± 131	151 ± 101	106 ± 104
Mg	104 ± 100	278 ± 255	278 ± 294	209 ± 235
Al	478 ± 421	1225 ± 1123	1165 ± 1408	913 ± 1056
Si	1097 ± 997	2903 ± 2792	2558 ± 3408	2103 ± 2571
K	608 ± 347	1356 ± 692	2884 ± 1883	1413 ± 1343
Ca	1746 ± 1531	4454 ± 3821	4256 ± 5894	3329 ± 3992
V	5.9 ± 4.3	8.3 ± 6.1	11 ± 8.0	7.9 ± 6.2
Ni	2.3 ± 1.7	4.0 ± 2.7	3.9 ± 3.5	3.3 ± 2.7
Cu	13 ± 10	22 ± 13	36 ± 22	22 ± 17
Zn	95 ± 145	162 ± 134	275 ± 161	162 ± 160
As	5.9 ± 6.4	12 ± 6.6	26 ± 18	13 ± 13
Se	3.9 ± 3.1	6.6 ± 2.9	15 ± 9.3	7.4 ± 6.6
Sb	13 ± 8.8	23 ± 13	38 ± 20	23 ± 17
Ba	16 ± 16	35 ± 31	109 ± 147	45 ± 82
Pb	44 ± 27	71 ± 27	165 ± 68	82 ± 62
Cr	4.7 ± 4.4	8.7 ± 5.4	12 ± 7.8	7.9 ± 6.3
Mn	31 ± 29	66 ± 45	85 ± 62	56 ± 49
Fe	647 ± 539	1788 ± 1795	1852 ± 2319	1348 ± 1691
Cl	387 ± 410	862 ± 548	2772 ± 1568	1117 ± 1272
Ti	59 ± 53	153 ± 150	145 ± 192	114 ± 140

components in $PM_{2.5}$ increased continuously and noticeably with the aggravation of pollution. Especially, the OM, NO_3^-, and Cl^- concentrations on NP, MP, and HP days were 62, 50, and 7.3 μg/m^3, respectively, and these values were 5.4–12.3 and 2.6–4.0 times as high as they were on NP and MP days, respectively. Hence, the formation of HP days was related to the increase in the contribution of all components.

Source apportionment

In this study, based on PMF modeling results, the number of sources was set from four to nine to find the minimum value of Q and make the value of residual matrix E as small as possible. Finally, six factors were chosen for PMF analysis (Fig. 4). The result was constrained with $d_{Qrobust}$ of 0.6%, and F_{peak} = 0.0 was selected as the optimal solution because of the increasing Q value without optimizing the source profiles (Table S5).

The six sources are shown in Fig. 4: (1) dust as signified by the dominant presence of Ca, Si, Al, Mg, Ti, Fe, and Mn (Almeida et al. 2008; Tullio et al. 2008; Liu et al. 2016); (2) vehicle traffic indicated by a high loading of Zn, V, Cu, Ni, and Mn (Canha et al. 2012; Shafer et al. 2012; Lin et al. 2015); (3) coal combustion heavily weighted by As, Cl^-, EC, Pb, and OC (Bhangare et al. 2011; Schleicher et al. 2011; Zheng et al. 2014; Khan et al. 2016; Liu et al. 2016); (4) secondary aerosols (SAs) suggested by the dominant presence of NO_3^-, NH_4^+, SO_4^{2-}, and OC (Wang et al. 2006; Srimuruganandam and Nagendra 2012; Tao et al. 2013; Liu et al. 2015); (5) industrial processes characterized by high loadings of Cr, Se, and Ni (López et al. 2011; Morishita et al. 2011; Almeida et al.

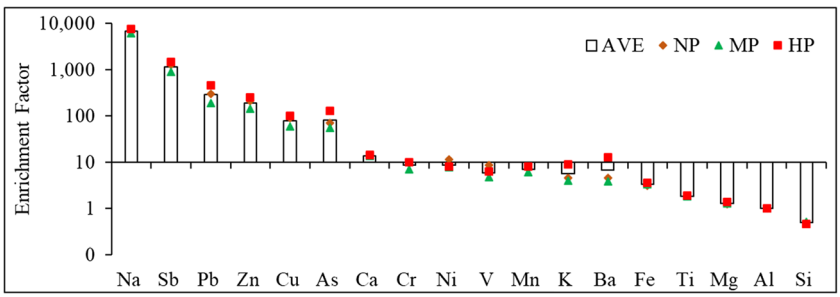

Fig. 2 Enrichment factors of the elements in $PM_{2.5}$ during different pollution levels at all sites in Zhengzhou

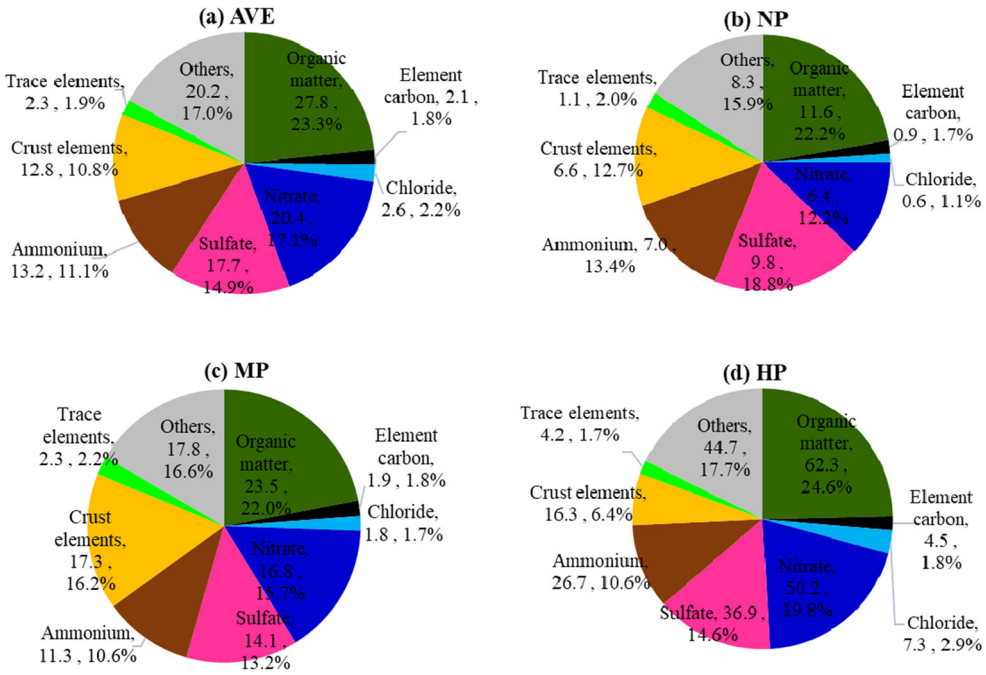

Fig. 3 Pie charts depicting the relative concentrations (μg/m^3) and contribution (%) of major chemical components of gravimetric $PM_{2.5}$ based on annual data at all sites in Zhengzhou

2015; Yao et al. 2016); and (6) biomass burning mainly weighted by Cl^-, OC, EC, and K (Heo et al. 2009; Hleis et al. 2013; Almeida et al. 2015).

Figure 5 shows the source contributions (%) and concentrations (μg/m^3) of the identified sources to $PM_{2.5}$ mass. Generally, SAs had the highest contribution (35.1%) to $PM_{2.5}$ mass concentration during the sampling period probably because of an intensive secondary reaction. The wet desulfurization of coal-fired power plants can directly discharge sulfate particles into the air to a certain extent (Ma et al. 2015). Coal combustion (17.6%) and vehicle traffic (17.3%) were also major sources contributed to ambient $PM_{2.5}$ in Zhengzhou. The contributions of industrial processes, dust, and biomass burning sources on $PM_{2.5}$ were 7.3%, 15.1%, and 7.7%, respectively. During the transition from NP days to HP days, SAs concentration was 6.3 times higher on HP days (97 μg/m^3) than on NP days (15 μg/m^3). The highest contribution of SAs on HP days attributed to the low

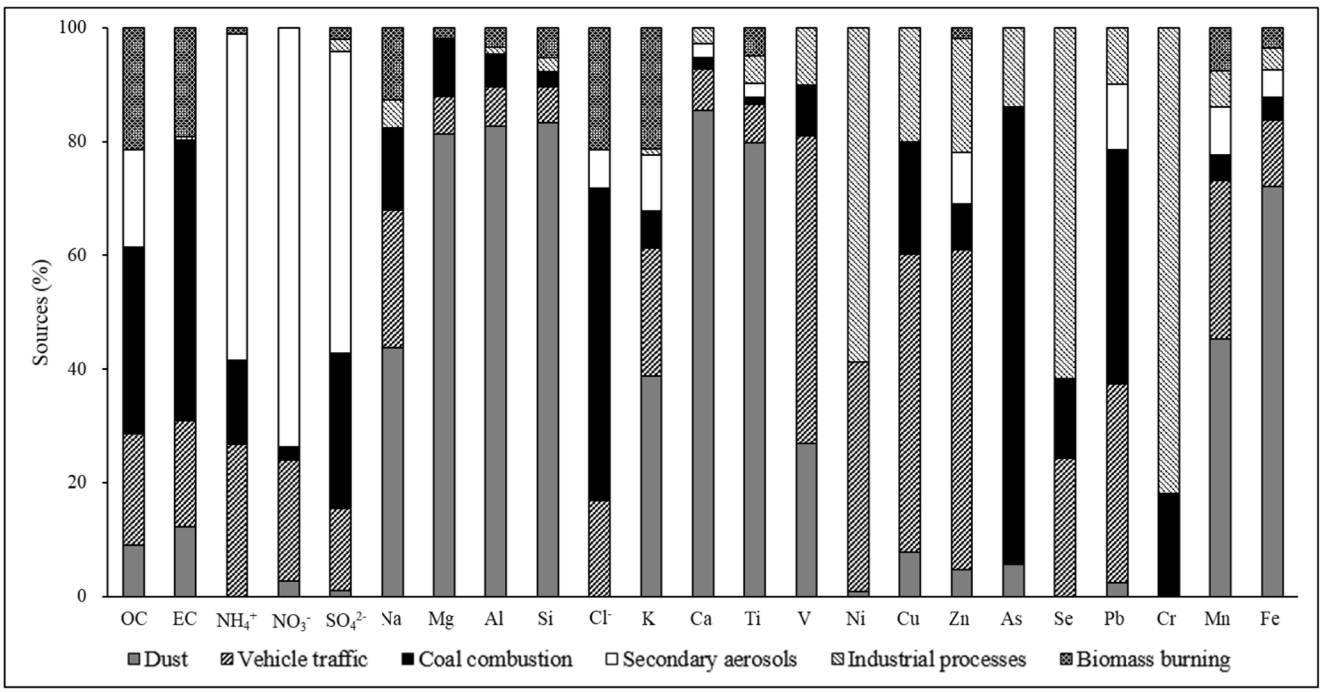

Fig. 4 Source contributions (%) for each species (by mass) (all sites and all pollution levels)

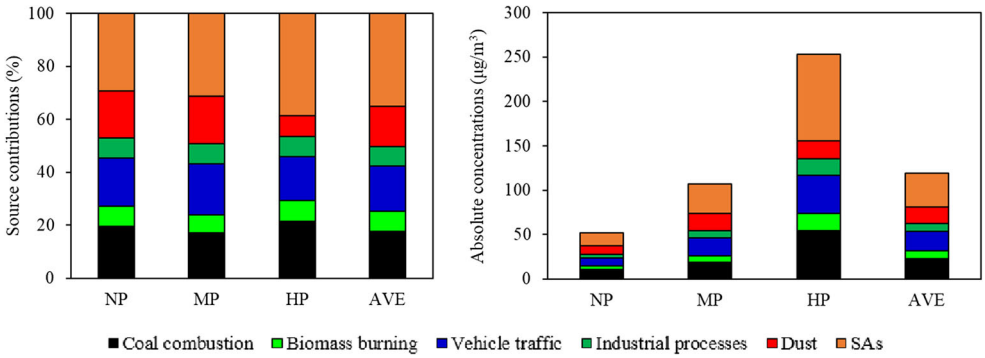

Fig. 5 The annual contributions (%) and absolute concentrations (μg/m^3) of identified sources to $PM_{2.5}$ mass on different pollution levels at all sites in Zhengzhou

temperature, high humidity, and low planetary boundary layer in polluted days were conducive to the formation of secondary particles (Ogulei et al. 2006; Kim and Hopke 2008; Jiang et al. 2018d). The concentration of coal combustion rose from 10 μg/m^3 on NP days to 18 μg/m^3 on MP days and 55 μg/m^3 on HP days, implying that the impact of coal combustion was enhanced with the aggravation of $PM_{2.5}$ pollutions. The contributions of dust source on HP days decreased, indicating a relatively low influence on the aggravation of $PM_{2.5}$ pollutions. Furthermore, the contribution of biomass burning and industrial process sources varied slightly at different pollution levels. In brief, SAs and coal combustion played important roles in high $PM_{2.5}$ pollution, and the government should strengthen the control of precursor (SO_2, NO_X, NH_3, and VOCs) emissions and coal combustion sources to mitigate heavy pollution levels.

The fractional contribution of sources to $PM_{2.5}$ mass at different pollution levels during the study period at the five sites is shown in Fig. S6. The SAs has the highest contribution to $PM_{2.5}$ mass concentration at each sampling site, with contribution ranging from 33.2% (HKG) to 42.0% (DF). Specifically, the contribution of SAs on HP days was 34.8% (ZM) to 59.8% (DF), and the contribution of SAs absolute concentration was 86 μg/m^3 (XM) to 172 μg/m^3 (DF). In addition, the common feature of each site was that the contribution of SAs on HP days was higher than that on NP and MP days. Coal combustion was one of the major sources of ambient $PM_{2.5}$ at each sampling site. At the XM sites, the coal combustion source exhibited significantly high contributions to $PM_{2.5}$ (20.4%), especially on HP days when its contribution accounted for 25.2%, which was likely associated with emissions from coal-fired burning industry because the XM site is an industrial site. The lowest contribution of coal combustion was recorded at the HKG (15.9%) site, which has relatively few factories nearby. SSQ site is located in a busy business district with heavy traffic, so the vehicle traffic (22.1%) proportion was highest. Furthermore, the HKG site is close to the Xinzheng International Airport. Considering the influence of jet fuel and vehicle, the traffic source contribution of the HKG site was higher (18.6%) than that of the three other sites. For industrial processes source, the contribution of this factor at the XM site (an industrial site, 11.4%, 14 μg/m^3) was higher than that at the other sites. For dust source, relatively high contributions were observed at SSQ and HKG sites, whereas relatively low contribution was observed at DF site, which is a scenic site. For biomass burning source, the highest contribution was recorded at ZM site, which is an agricultural site, probably due to open burning of straws and the use of straws as energy for cooking food and heating in rural areas.

Source analysis based on backward trajectories

The backward trajectory cluster of source contributions at different pollution levels is shown in Fig. 6. On NP days, 93.8% of the air mass (cluster 1) as close-range transport was mainly from Zhumadian in Henan Province, with an average $PM_{2.5}$ of 58 μg/m^3. Cluster 2 (6.3%) as the middle-range transport originated from Fuyang in Anhui Province, with an average $PM_{2.5}$ of 53 μg/m^3. On MP days, all air masses came from the northwest, with middle-range transport (cluster 2) from Shanxi Province (14.6%, 104 μg/m^3) and long-range transport (cluster 1) from Shaanxi Province (85.4%, 107 μg/m^3). However, on HP days, 65.6% of the air mass (cluster 2) as close-range transport mainly came from Zhoukou in Henan Province, with a high $PM_{2.5}$ level (284 μg/m^3). Cluster 1 as long-range transport originated from Mongolia (6.3%) and passed over Inner Mongolia, Shaanxi, and Shanxi, with an average $PM_{2.5}$ of 209 μg/m^3. Therefore, close-range transport was still one of the dominant factors for HP days in Zhengzhou.

In addition to different $PM_{2.5}$ concentrations in different clusters, significant differences were observed in the proportion of its source contribution (Fig. 6). On NP days, the contributions of SAs, dust, vehicle traffic, and industrial processes in cluster 1 were higher than those in cluster 2. By contrast, the contributions of coal combustion and biomass burning sources exhibited an opposite pattern. SAs (54.9%, much higher than the value at SSQ site from PMF, Fig. S6, 32.6%) contribution of cluster 1 was the highest, and the coal combustion (37.1%) contribution of cluster 2 was the highest. Therefore, the air mass transport from Zhumadian and Fuyang is important for SAs and coal combustion on NP days,

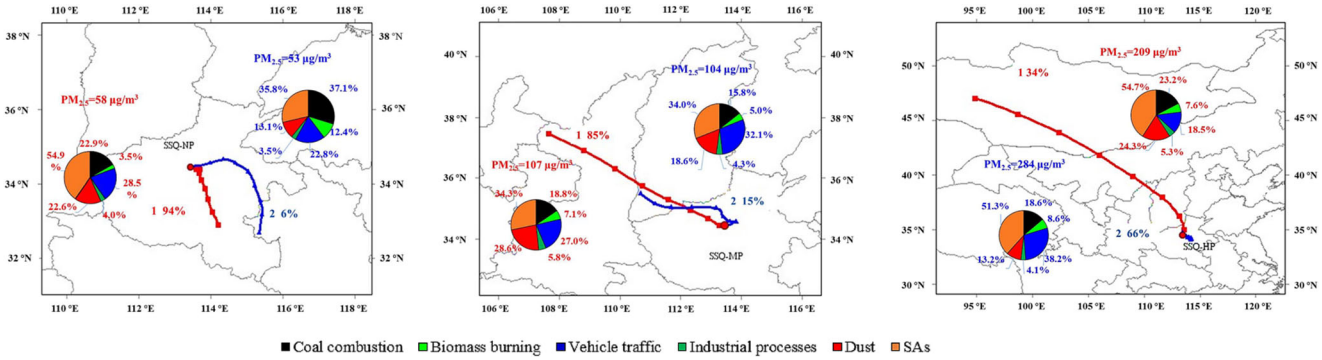

Fig. 6 Source contributions resolved from the PMF at each 48 h backward trajectory cluster during different pollution levels in Zhengzhou

respectively. On MP days, all sources except vehicle traffic contributed to cluster 1 > cluster 2, and the contribution of air mass cluster 1 mainly comes from dust (28.6%) and SAs (34.3%), while cluster 2 mainly comes from vehicle traffic (32.1%) and SAs (34.0%). Therefore, the air masses from northwest bring relative high dust, SAs, and vehicle traffic contribution on MP days. On HP days, the contribution of SAs, dust, coal combustion, and industrial processes in cluster 1 was higher than that in cluster 2, while the contribution of vehicle traffic and biomass burning sources in cluster 2 was higher than that in cluster 1. The contribution of dust (24.3%) and SAs (54.7%) in cluster 1 is relatively high. These pollution sources originate from northwest direction passing by the Gobi Desert to the sampling site through long-distance transmission. Vehicle traffic (38.2%) and SAs (51.3%) in cluster 2 have a relative high contribution, mainly coming from short-distance transmission.

Potential contribution source areas of $PM_{2.5}$

Figures 7 and S7 present the potential source areas of $PM_{2.5}$ on NP, MP, and HP days at the SSQ site. Generally, the potential source areas were mainly located in Xinxiang, Kaifeng, Xuchang, Pingdingshan, and Luoyang and distributed to the east, west, and south of Zhengzhou. On NP, MP, and HP days, the areas with high-weighted WPSCF values of $PM_{2.5}$ (> 0.6) differed, and the areas were Pingdingshan and Kaifeng on NP days, Kaifeng and Xuchang on MP days, and Luoyang and Kaifeng on HP days.

The PSCF analysis of $PM_{2.5}$ sources on NP, MP, and HP days are displayed in Figs. 8 and S8. On NP days, the potential source areas of coal combustion, biomass burning, dust, and SAs were found in Pingdingshan, Xinxiang, and Kaifeng. The potential source regions of vehicle traffic and industrial processes were scattered across Pingdingshan and Xuchang. On MP days, high WPSCF values of coal combustion were distributed in Xinxiang, Xuchang, Luohe, Zhumadian, and Pingdingshan, and high WPSCF values of other sources were mainly distributed in Xuchang, Luohe, and Kaifeng. On HP days, the potential regions of coal combustion, biomass burning, vehicle traffic, and industrial processes sources come from Kaifeng and Xinxiang, which are two cities with large amounts of emissions of industrial coal. Dust and SAs mainly originated from Pingdingshan and Kaifeng. Pingdingshan is the largest coal-producing city in Henan Province, and agriculture is flourishing in Kaifeng (Bureau of Statistics of Henan Province 2017), and the processes of mining and farming emits a large amount of dust.

Health risks of elements

CR values from 1×10^{-6} to 1×10^{-4} indicate a tolerable risk, while CR values above 1×10^{-4} are intolerable. For non-carcinogenic risk, HQ (HI) > 1 indicates a significant risk for each element (total elements) (US EPA 1989). The carcinogenic and non-carcinogenic risks of toxic elements in $PM_{2.5}$ on different pollution days through the three exposure pathways are shown in Tables 5 and S6–S8.

The CR values of Pb, As, and Ni for children and adults ranged from 8.5×10^{-7} to 3.5×10^{-6}, from 2.8×10^{-5} to 8.4×10^{-5}, and from 9.7×10^{-6} to 6.9×10^{-5}, respectively, showing a tolerable risk for each element. The total CR values through the three exposure pathways were higher than 1.0×10^{-4} for children on NP and MP days, suggesting an intolerable risk. An AEA (2011) research showed that As mainly comes from the production of metals and public electricity and heat, while Ni mainly comes from heavy fuel oil combustion. Therefore, local regulators should strengthen the management and control of emissions from these sources (i.e., coal-fired power plants, metal production, and non-road mobile sources) to reduce As and Ni levels. The non-carcinogenic risks of As (1.4–2.3) for children on different pollution days and the value of Pb (1.0–1.4) for children on NP and MP days were higher than 1, indicating significant risks. Although the use of leaded gasoline has been banned since 2000, reducing lead emissions from motor vehicles, lead aerosols in the atmosphere still come mainly from man-made sources (Widory 2006), e.g., the main source of lead in Zhengzhou was coal combustion,

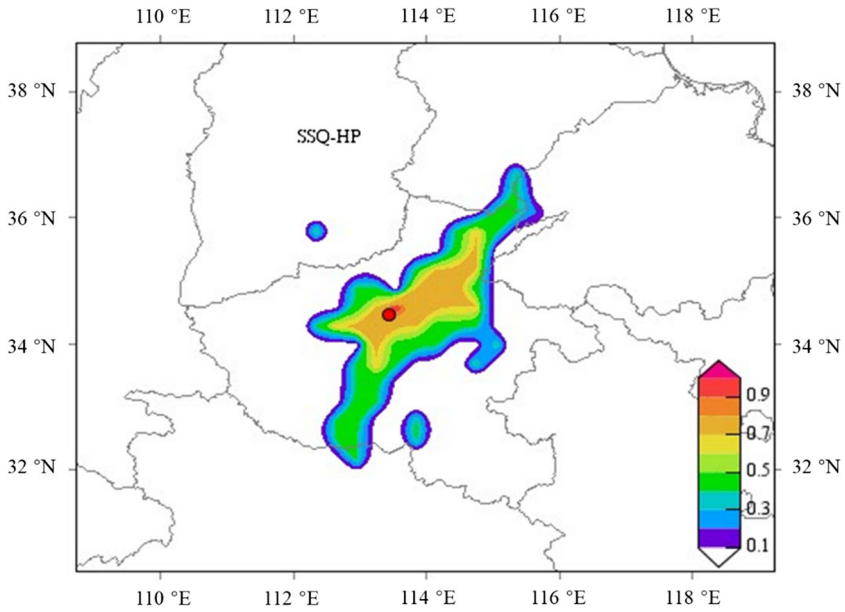

Fig. 7 PSCF analysis of $PM_{2.5}$ in HP days (the color legend represented to the WPSCF value)

which has a significant impact on human health. The non-carcinogenic risks of total toxic elements were above 1 for children at the three pollution levels, indicating an intolerable risk. Therefore, children with higher CR and HQ values were more sensitive than adults.

Generally, the intake pathway had the highest risk of the three exposure pathways. In the intake pathway, for As, with CR values ranging from 2.5×10^{-5} to 8.1×10^{-5} on different pollution days. The CR values of total toxic elements exceeded 1.0×10^{-4} for children on NP and MP days, indicating an intolerable carcinogenic risk. The HI values ranged from 2.1 to 4.0 for children through the daily intake pathway during different pollution days, indicating an intolerable risk. In this pathway, the HQ values of As element at the three pollution levels for children and Pb on NP days for children were all over 1, indicating intolerable risks. Although the total CR and HI values of HP days were generally smaller than those of NP and MP days because of the least number of HP days, the average daily non-carcinogenic and carcinogenic risks of toxic elements on HP days were still greater than those on NP and MP days.

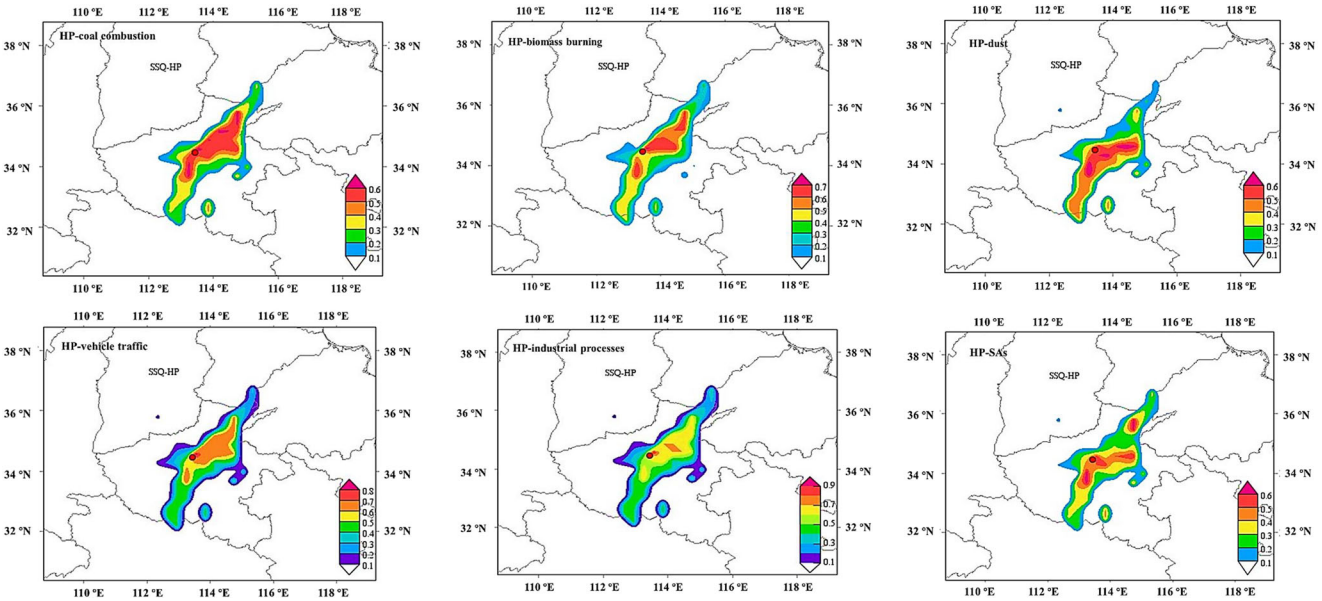

Fig. 8 PSCF analysis based on sources of coal combustion, biomass burning, vehicle traffic, industrial processes, dust, and SAs of $PM_{2.5}$ in HP days (the color legend represented to the WPSCF value)

Table 5 Carcinogenic and non-carcinogenic risks for each element in $PM_{2.5}$ through three pathways in different pollution levels during the entire sampling period at all sites in Zhengzhou

NP			MP			HP		
Toxic elements	Carcinogenic risk (CR) Child	Carcinogenic risk (CR) Adult	Toxic elements	Carcinogenic risk (CR) Child	Carcinogenic risk (CR) Adult	Toxic elements	Carcinogenic risk (CR) Child	Carcinogenic risk (CR) Adult
As	8.4E−05	4.4E−05	As	7.6E−05	4.0E−05	As	5.0E−05	2.8E−05
Pb	3.5E−06	1.8E−06	Pb	2.4E−06	1.3E−06	Pb	1.6E−06	8.5E−07
Ni	6.9E−05	4.1E−05	Ni	4.6E−05	2.7E−05	Ni	1.6E−05	9.7E−06
CR	1.6E−04	8.7E−05	CR	1.2E−04	6.9E−05	CR	6.8E−05	3.8E−05
Toxic elements	Non-carcinogenic risk Child	Non-carcinogenic risk Adult	Toxic elements	Non-carcinogenic risk Child	Non-carcinogenic risk Adult	Toxic elements	Non-carcinogenic risk Child	Non-carcinogenic risk Adult
V	2.8E−01	5.1E−02	V	1.7E−01	3.4E−02	V	7.3E−02	1.8E−02
Cu	3.9E−02	5.0E−03	Cu	2.8E−02	3.6E−03	Cu	1.4E−02	1.8E−03
As	2.3E+00	3.4E−01	As	2.1E+00	3.4E−01	As	1.4E+00	2.9E−01
Mn	2.5E−01	1.1E−01	Mn	2.3E−01	1.7E−01	Mn	1.0E−01	1.3E−01
Zn	4.1E−02	5.2E−03	Zn	3.0E−02	3.9E−03	Zn	1.3E−02	1.7E−03
Pb	1.4E+00	1.8E−01	Pb	1.0E+00	1.3E−01	Pb	6.5E−01	8.4E−02
Ni	4.6E−02	1.2E−02	Ni	3.0E−02	1.3E−02	Ni	1.1E−02	6.9E−03
HI	4.1E+00	7.0E−01	HI	3.4E+00	6.9E−01	HI	2.1E+00	5.3E−01

Conclusions

In this study, the chemical compositions and emission sources of $PM_{2.5}$ in Zhengzhou were comprehensively investigated. The annual mean concentration of $PM_{2.5}$ was 119 μg/m^3 in Zhengzhou. Heavily polluted days mainly occurred in winter, while non-polluted days mainly occurred in summer. The average concentration of $PM_{2.5}$ in Zhengzhou on NP, MP, and HP days were 52, 107, and 253 μg/m^3, respectively. The carbonaceous species, WSIIs, and elements had contributions of 25%, 50%, and 10% to $PM_{2.5}$, respectively. The OC/EC mean ratios of 8.2, 7.6, and 9.8 were recorded on NP, MP, and HP days, respectively. This finding indicated that more secondary organic matter was produced on HP days than on the other days, and secondary formation might enhance weather pollution. Both conditions increased the NOR and SOR as the pollution degree increased. Na, Sb, Pb, Zn, Cu, and As were closely related to anthropogenic activities, while Al, Si, Mg, Fe, and Ti mainly came from crustal sources.

The PMF model revealed that SAs, coal combustion, vehicle traffic, industrial processes, dust, and biomass burning were the main sources of $PM_{2.5}$ in Zhengzhou. The SAs had the highest contributions during every pollution levels. Although the SAs contribution was 1.3 times higher on HP days than on NP days, SAs concentration was 6.3 times higher on HP days (97 μg/m^3) than on NP days (15 μg/m^3).

Backward trajectory cluster analysis showed that the transport of pollutants in Zhengzhou mainly came from Zhumadian and Zhoukou in Henan Province, Fuyang in Anhui Province, Shanxi, Shaanxi, Mongolia, and Inner Mongolia. On HP day, the main contributor to air quality transmission pollution was SAs. The PSCF analysis identified Xuchang, Pingdingshan, Luohe, Zhumadian, Xinxiang, and Kaifeng as the potential regions of $PM_{2.5}$ pollutant sources.

The non-carcinogenic and carcinogenic risk values of toxic elements from all sites during different pollution levels through the three pathways were higher in children than in adults. Among the three exposure pathways, the daily intake had the highest risk. Significant risks existed in the non-carcinogenic risk of As (1.4–2.3) for children at three pollution levels and the non-carcinogenic risk of Pb (1.0–1.4) for children with NP and MP. The average daily non-carcinogenic and carcinogenic risks of toxic elements on HP days were greater than those on the other days.

Author's contributions NJ, RZ, and SL conceived and designed the study; XL analyzed the date and wrote the paper; XY and QM performed aerosol sampling and date analyses.

Funding The study was supported by the financial support from the National Natural Science Foundation of China (51808510, 51778587), National Key Research and Development Program of China (2017YFC0212400), and Natural Science Foundation of Henan Province of China (162300410255).

Data availability The datasets used during the current study are available from the corresponding author on reasonable request (jiangn@zzu.edu.cn).

Compliance with ethical standards

Ethics approval Not applicable

Consent to participate Not applicable

Consent for publication Not applicable

Competing interests The authors declare that they have no competing interests.

References

AEA (2011) UK emissions of air pollutants 1970 to 2009. UK Emissions Inventory Team, Department for Environment, Food and Rural Affairs. http://ukair.defra.gov.uk/reports/cat07/1401131501_NAEI_Annual_Report_2009.pdf. Accessed 22 December 2019

Almeida SM, Freitas MC, Pio CA (2008) Neutron activation analysis for identification of African mineral dust transport. Radioanal Nucl Chem 276:161–165. https://doi.org/10.1007/s10967-007-0426-4

Almeida SM, Lage J, Fernandez B, Garcia S, Reis MA, Chaves PC (2015) Chemical characterization of atmospheric particles and source apportionment in the vicinity of a steelmaking industry. Sci Total Environ 521-522:411–420. https://doi.org/10.1016/j.scitotenv.2015.03.112

Andreae MO, Rosenfeld D (2008) Aerosol–cloud–precipitation interactions. part 1. The nature and sources of cloud-active aerosols. Earth Sci Rev 89:13–41. https://doi.org/10.1016/j.earscirev.2008.03.001

Bhangare RC, Ajmal PY, Sahu SK, Pandit GG, Puranik VD (2011) Distribution of trace elements in coal and combustion residues from five thermal power plants in India. Int J Coal Geol 86:349–356. https://doi.org/10.1016/j.coal.2011.03.008

Bureau of Statistics of Henan Province (2017) Henan Statistical Yearbook 2017. China Statistics Press, Beijing (in Chinese). http://www.ha.stats.gov.cn/hntj/lib/tjnj/2017/indexch.htm. Accessed 20 December 2019

Bureau of Statistics of Zhengzhou (2017) Statistical Bulletins on National Economic and Social Development of Zhengzhou in 2016 (in Chinese). http://tjj.zhengzhou.gov.cn/tjgb/418270.jhtml. Accessed 25 December 2019

Cakmak S, Dales R, Kauri LM, Mahmud M, Van Ryswyk K, Vanos J, Liu L, Kumarathasan P, Thomson E, Vincent R, Weichenthal S (2014) Metal composition of fine particulate air pollution and acute changes in cardiorespiratory physiology. Environ Pollut 189:208–214. https://doi.org/10.1016/j.envpol.2014.03.004

Canha N, Freitas MC, Almeida-Silva M, Almeida SM, Dung HM, Dionísio I, Cardoso J, Pio CA, Caseiro A, Verburg TG, Wolterbeek HT (2012) Burn wood influence on outdoor air quality in a small village: foros de Arrao, Portugal. Radioanal Nucl Chem 291:83–88. https://doi.org/10.1007/s10967-011-1261-1

Cao JJ, Wu F, Chow JC, Lee SC (2005) Characterization and source apportionment of atmospheric organic and elemental carbon during fall and winter of 2003 in Xi'an, China. Atmos Chem Phys 5(11):3127–3137. https://doi.org/10.5194/acp-5-3127-2005

Chen J, Wei F, Zheng C, Wu Y, Adriano DC (1991) Background concentrations of elements in soils of China. Water Air Soil Pollut 57-58:699–712. https://doi.org/10.1007/BF00282934

Chen Y, Zhi G, Feng Y, Fu J, Feng J, Sheng G, Simoneit BRT (2006) Measurements of emission factors for primary carbonaceous particles from residential raw-coal combustion in China. Geophys Res Lett 33:L20815. https://doi.org/10.1029/2006gl026966

Chen ZY, Cai J, Gao BB, Xu B, Dai S, He B, Xie XM (2017) Detecting the causality influence of individual meteorological factors on local $PM_{2.5}$ concentration in the Jing-Jin-Ji region. Sci Rep 7:40735. https://doi.org/10.1038/srep40735

Chow JC, Watson JG, Lu Z, Lowenthal DH, Frazier CA, Solomon PA, Thuillier RH, Magliano K (1996) Descriptive analysis of $PM_{2.5}$ and PM_{10} at regionally representative locations during SJVAQS/AUSPEX. Atmos Environ 30:2079–2112. https://doi.org/10.1016/1352-2310(95)00402-5

Chow JC, Bachmann JD, Wierman SSG, Mathai CV, Malm WC, White WH, Mueller PK, Kumar N, Watson JG (2002) Visibility: science and regulation. J Air Waste Manage Assoc 52:973–999. https://doi.org/10.1080/10473289.2002.10470844

Coyle YM, Minahjuddin AT, Hynan LS, Minna JD (2006) An ecological study of the association of metal air pollutants with lung cancer incidence in Texas. J Thorac Oncol 1:654–661. https://doi.org/10.1016/s1556-0864(15)30377-4

Dai QL, Bi XH, Liu BS, Li LW, Ding J, Song WB, Bi SY, Schulze BC, Song CB, Wu JH, Zhang YF, Feng YC, Hopke PK (2018) Chemical nature of $PM_{2.5}$ and PM_{10} in Xi'an, China: Insights into primary emissions and secondary particle formation. Environ Pollut 240:155–166. https://doi.org/10.1016/j.envpol.2018.04.111

Feng JL, Yu H, Mi K, Su XF, Li Y, Li QL, Sun JH (2018) One year study of $PM_{2.5}$ in Xinxiang city, North China: seasonal characteristics, climate impact and source. Ecotoxicol Environ Saf 154:75–83. https://doi.org/10.1016/j.ecoenv.2018.01.048

Fu QY, Zhuang GS, Wang J, Xu C, Huang K, Li J, Hou B, Lu T, Streets DG (2008) Mechanism of formation of the heaviest pollution episode ever recorded in the Yangtze River Delta, China. Atmos Environ 42:2023–2036. https://doi.org/10.1016/j.atmosenv.2007.12.002

Gildemeister AE, Hopke PK, Kim EG (2007) Sources of fine urban particulate matter in Detroit, MI. Chemosphere 69:1064–1074. https://doi.org/10.1016/j.chemosphere.2007.04.027

Han Y, Kim H, Cho S, Kim P, Kim W (2015) Metallic elements in $PM_{2.5}$ in different functional areas of Korea: concentrations and source identification. Atmos Res 153:416–428. https://doi.org/10.1016/j.atmosres.2014.10.002

Heo JB, Hopke P, Yi SM (2009) Source apportionment of $PM_{2.5}$ in Seoul, Korea. Atmos Chem Phys 9:4957–4971. https://doi.org/10.5194/acpd-8-20427-2008

Hleis D, Fernandez-Olmo I, Ledoux F, Kfoury A, Courcot L, Desmonts T, Courcot D (2013) Chemical profile identification of fugitive and confined particle emissions from an integrated iron and steel making plant. J Hazard Mater 250-251:246–255. https://doi.org/10.1016/j.jhazmat.2013.01.080

Hsu CY, Chiang HC, Lin SL, Chen MJ, Lin TY, Chen YC (2016) Elemental characterization and source apportionment of PM_{10} and $PM_{2.5}$ in the western coastal area of central Taiwan. Sci Total Environ 541:1139–1150. https://doi.org/10.1016/j.scitotenv.2015.09.122

Huang XJ, Liu ZR, Zhang JK, Wen TX, Ji DS, Wang YS (2016) Seasonal variation and secondary formation of size-segregated aerosol water-soluble inorganic ions during pollution episodes in Beijing. Atmos Res 168:70–79. https://doi.org/10.1016/j.atmosres.2015.08.021

Huang XJ, Liu ZR, Liu JY, Hu B, Wen TX, Tang GQ, Zhang JK, Wu FK, Ji DS, Wang LL, Wang YS (2017) Chemical characterization and synergetic source apportionment of $PM_{2.5}$ at multiple sites in the Beijing-Tianjin-Hebei region, China. Atmos Chem Phys 17(21):1–34. https://doi.org/10.5194/acp-2017-446

Jiang N, Guo Y, Wang Q, Kang PR, Zhang RQ, Tang XY (2017) Chemical composition characteristics of $PM_{2.5}$ in three cities in

Henan, central China. Aerosol Air Qual Res 17:2367–2380. https://doi.org/10.4209/aaqr.2016.10.0463

Jiang N, Li Q, Su FC, Wang Q, Yu X, Kang PR, Zhang RQ, Tang XY (2018a) Chemical characteristics and source apportionment of $PM_{2.5}$, between heavily polluted days and other days in Zhengzhou, China. Environ Sci 66:188–198. https://doi.org/10.1016/j.jes.2017.05.006

Jiang N, Yin SS, Guo Y, Li JY, Kang PR, Zhang RQ, Tang XY (2018b) Characteristics of mass concentration, chemical composition, source apportionment of $PM_{2.5}$ and PM_{10} and health risk assessment in the emerging megacity in China. Atmos Pollut Res 9:309–321. https://doi.org/10.1016/j.apr.2017.07.005

Jiang N, Dong Z, Xu YQ, Yu F, Yin SS, Zhang RQ, Tang XY (2018c) Characterization of PM_{10} and $PM_{2.5}$ source profiles for fugitive dust in Zhengzhou, China. Aerosol Air Qual Res 18:314–329. https://doi.org/10.1016/S1352-2310(02)01028-2

Jiang N, Duan SG, Yu X, Zhang RQ, Wang K (2018d) Comparative major components and health risks of toxic elements and polycyclic aromatic hydrocarbons of $PM_{2.5}$ in winter and summer in Zhengzhou: Based on three-year data. Atmos Res 213:173–184. https://doi.org/10.1016/j.atmosres.2018.06.008

Jiang N, Liu XH, Wang SS, Yu X, Yin SS, Duan SG, Wang SB, Zhang RQ, Li SL (2019) Pollution characterization, source identification, and health risks of atmospheric-particle-bound heavy metals in PM_{10} and $PM_{2.5}$ at multiple sites in an emerging megacity in the central region of China. Aerosol Air Qual Res 19:247–271. https://doi.org/10.4209/aaqr.2018.07.0275

Khan MF, Latif MT, Saw WH, Amil N, Nadzir MSM, Sahani M, Tahir NM, Chung JX (2016) Fine particulate matter in the tropical environment: monsoonal effects, source apportionment, and health risk assessment. Atmos Chem Phys 16:597–617. https://doi.org/10.5194/acp-16-597-2016

Kim EG, Hopke PK (2008) Source characterization of ambient fine particles at multiple sites in the Seattle area. Atmos Environ 42:6047–6056. https://doi.org/10.1016/j.atmosenv.2008.03.032

Li Q, Jiang N, Yu X, Dong Z, Duan SG, Zhang RQ (2019) Sources and spatial distribution of $PM_{2.5}$-bound polycyclic aromatic hydrocarbons in Zhengzhou in 2016. Atmos Res 216:65–75. https://doi.org/10.1016/j.atmosres.2018.09.011

Liang CS, Duan FK, He KB, Ma YL (2016) Review on recent progress in observations, source identifications and countermeasures of $PM_{2.5}$. Environ Int 86:150–170. https://doi.org/10.1016/j.envint.2015.10.016

Lin YC, Tsai CJ, Wu YC, Zhang R, Chi KH, Huang YT, Lin SH, Hsu SC (2015) Characteristics of trace metals in traffic-derived particles in Hsuehshan Tunnel, Taiwan: size distribution, potential source, and finger printing metal ratio. Atmos Chem Phys 15:4117–4130. https://doi.org/10.5194/acp-15-4117-2015

Liu JW, Li J, Zhang YL, Liu D, Ding P, Shen CD, Shen KJ, He QF, Ding X, Wang XM, Chen DH, Szidat S, Zhang G (2014) Source apportionment using radiocarbon and organic tracers for $PM_{2.5}$ carbonaceous aerosols in Guangzhou, South China: contrasting local- and regional-scale haze events. Environ Sci Technol 48:12002–12011. https://doi.org/10.1021/es503102w

Liu G, Li JH, Wu D, Xu H (2015) Chemical composition and source apportionment of the ambient $PM_{2.5}$ in Hangzhou, China. Particuology 18:135–143. https://doi.org/10.1016/j.partic.2014.03.011

Liu BS, Song N, Dai QL, Mei RB, Sui BH, Bi XH, Feng YC (2016) Chemical composition and source apportionment of ambient $PM_{2.5}$ during the nonheating period in Taian, China. Atmos Res 170:23–33. https://doi.org/10.1016/j.atmosres.2015.11.002

Liu BS, Wu JH, Zhang JY, Wang L, Yang JM, Liang DN, Dai QL, Bi XH, Feng YC, Zhang YF, Zhang QX (2017) Characterization and source apportionment of $PM_{2.5}$ based on error estimation from EPA PMF 5.0 model at a medium city in China. Environ Pollut 222:10–22. https://doi.org/10.1016/j.envpol.2017.01.005

Liu B, Cheng Y, Zhou M, Liang D, Dai Q, Wang L, Jin W, Zhang L, Ren Y, Zhou J, Dai C, Xu J, Wang J, Feng Y, Zhang Y (2018) Effectiveness evaluation of temporary emission control action in 2016 in winter in Shijiazhuang, China. Atmos Chem Phys 18:7019–7039. https://doi.org/10.5194/acp-2017-1001

Liu XH, Jiang N, Yu X, Zhang RQ, Li SL, Li Q, Kang PR (2019) Chemical characteristics, sources apportionment, and risk assessment of $PM_{2.5}$ in different functional areas of an emerging megacity in China. Aerosol Air Qual Res 19:2222–2238. https://doi.org/10.4209/aaqr.2019.02.0076

López ML, Ceppi S, Palancar GG, Olcese LE, Tirao G, Toselli BM (2011) Elemental concentration and source identification of PM_{10} and $PM_{2.5}$ by SR-XRF in Córdoba City, Argentina. Atmos Environ 45:5450–5457. https://doi.org/10.1016/j.atmosenv.2011.07.003

Lough GC, Schauer JJ, Park JS, Shafer MM, DeMinter JT, Weinstein JP (2004) Emissions of metals associated with motor vehicle roadways. Environ Sci Technol 39:826–836. https://doi.org/10.1021/es048715f

Ma ZZ, Li Z, Jiang JK, Ye ZX, Deng JG, Duan L (2015) Characteristics of water-soluble inorganic ions in $PM_{2.5}$ emitted from coal-fired power plants. Environ Sci. (in Chinese) 36:2361–2366. https://doi.org/10.13227/j.hjkx.2015.03.047

Manousakas M, Papaefthymiou H, Diapouli E, Migliori A, Karydas AG, Bogdanovic-Radovic I, Bogdanovic-Radovic K (2017) Assessment of $PM_{2.5}$ sources and their corresponding level of uncertainty in a coastal urban area using EPA PMF 5.0 enhanced diagnostics. Sci Total Environ 574:155–164. https://doi.org/10.1016/j.scitotenv.2016.09.047

Ministry of Environmental Protection of the People's Republic of China (2012) Technical Regulation on Ambient Air Quality Index (on trial) http://bz.mee.gov.cn/bzwb/jcffbz/201203/t20120302_224166.shtml Accessed 20 December 2019

Morishita M, Gerald J, Keeler GJ, Kamal AS, Wagner JG, Harkem JR, Rohr AC (2011) Source identification of ambient $PM_{2.5}$ for inhalation exposure studies in Steubenville, Ohio using highly time-resolved measurements. Atmos Environ 45:7688–7697. https://doi.org/10.1016/j.atmosenv.2010.12.032

Nolting RF, Ramkema A, Everaarts JM (1999) The geochemistry of Cu, Cd, Zn, Ni and Pb in sediment cores from the continental slope of the Bancd' Arguin (Mauritania). Cont Shelf Res 19:665–691. https://doi.org/10.1016/s0278-4343(98)00109-5

Ogulei D, Hopke PK, Zhou JL, Paatero P, Park SS, John M (2005) Receptor modeling for multiple time resolved species: the Baltimore supersite. Atmos Environ 39:3751–3762. https://doi.org/10.1016/j.atmosenv.2005.03.012

Ogulei D, Hopke PK, Zhou JL, Pancras P, Nair N, Ondov JM (2006) Source apportionment of Baltimore aerosol from combined size distribution and chemical composition data. Atmos Environ 40:396–410. https://doi.org/10.1016/j.atmosenv.2005.11.075

Paatero P, Tapper U (1994) Positive matrix factorization: a non-negative factor model with optimal utilization of error estimates of data values. Environ Metrics 5:111–126. https://doi.org/10.1002/env.3170050203

Paatero P, Eberly S, Brown SG, Norris GA (2014) Methods for estimating uncertainty in factor analytic solutions. Atmos Meas Tech 7:781–797. https://doi.org/10.5194/amt-7-781-2014

Reff A, Eberly SI, Bhave PV (2007) Receptor modeling of ambient particulate matter data using positive matrix factorization: review of existing methods. J Air Waste Manage Assoc 57:146–154. https://doi.org/10.1080/10473289.2007.10465319

Rogula-Kozłowska W, Błaszczak B, Szopa S, Klejnowski K, Sowka I, Zwozdziak A, Jabłonska M, Mathews B (2013) $PM_{2.5}$ in the central part of Upper Silesia, Poland: concentrations, elemental

composition, and mobility of components. Environ Monit Assess 185:581–601. https://doi.org/10.1007/s10661-012-2577-1

Schauer JJ, Kleeman MJ, Cass GR, Simoneit BR (2002) Measurement of emissions from air pollution sources. 5. C1-C32 organic compounds from gasoline-powered motor vehicles. Environ Sci Technol 35: 1716–1728. https://doi.org/10.1021/es0108077

Schleicher NJ, Norra S, Chai F, Chen Y, Wang S, Cen K, Yu Y, Stueben D (2011) Temporal variability of trace metal mobility of urban particulate matter from Beijing-a contribution to health impact assessments of aerosols. Atmos Environ 45:7248–7265. https://doi.org/10.1016/j.atmosenv.2011.08.067

Shafer MM, Toner BM, Overdier JT, Schauer JJ, Fakra SC, Hu S, Herner JD, Ayala A (2012) Chemical speciation of vanadium in particulate matter emitted from diesel vehicles and urban atmospheric aerosols. Environ Sci Technol 46:189–195. https://doi.org/10.1021/es200463c

Simon H, Bhave PV, Swall JL, Frank NH, Malm WC (2011) Determining the spatial and seasonal variability in OM/OC ratios across the US using multiple regression. Atmos Chem Phys 11: 2933–2949. https://doi.org/10.5194/acp-11-2933-2011

Srimuruganandam B, Nagendra SMS (2012) Application of positive matrix factorization in characterization of PM_{10} and $PM_{2.5}$ emission sources at urban roadside. Chemosphere 88:120–130. https://doi.org/10.1016/j.chemosphere.2012.02.083

Subramanian R, Donahue NM, Bricker AB, Rogge WF, Robinson AL (2007) Insights into the primary–secondary and regional-local contribution to organic aerosol and $PM_{2.5}$ mass in Pittsburgh, Pennsylvania. Atmos Environ 41:7414–7433. https://doi.org/10.1016/j.atmosenv.2007.05.058

Tan J, Duan J, He K, Ma Y, Duan F, Chen Y, Fu J (2009) Chemical characteristics of $PM_{2.5}$ during a typical haze episode in Guangzhou. Environ Sci 21:774–781. https://doi.org/10.1016/s1001-0742(08)62340-2

Tang GQ, Zhang JQ, Zhu XW, Song T, Münkel C, Hu B, Schäfer K, Liu Z, Zhang JK, Wang LL, Xin JY, Suppan P, Wang YS (2016) Mixing layer height and its implications for air pollution over Beijing, China. Atmos Chem Phys 16:2459–2475. https://doi.org/10.5194/acp-16-2459-2016

Tao J, Cheng TT, Zhang RJ, Cao JJ, Zhu LH, Wang QY, Luo L, Zhang LM (2013) Chemical composition of $PM_{2.5}$ at an urban site of Chengdu in southwestern China. Adv Atmos Sci 30:1070–1084. https://doi.org/10.1007/s00376-012-2168-7

Tao J, Zhang LM, Ho KF, Zhang RJ, Lin ZJ, Zhang ZS, Lin M, Cao JJ, Liu SX, Wang GH (2014) Impact of $PM_{2.5}$ chemical compositions on aerosol light scattering in Guangzhou-the largest megacity in South China. Atmos Res 135-136:48–58. https://doi.org/10.1016/j.atmosres.2013.08.015

Tian YZ, Chen G, Wang HT, Huang-Fu YQ, Shi GL, Han B, Feng YC (2016) Source regional contributions to $PM_{2.5}$ in a megacity in China using an advanced source regional apportionment method. Chemosphere 147:256–263. https://doi.org/10.1016/j.chemosphere.2015.12.132

Tullio AD, Reale S, Ciammola M, Arrizza L, Picozzi P, De Angelis F (2008) Characterization of atmospheric particulate: relationship between chemical composition, size and emission source. ChemSusChem. 1:110–117. https://doi.org/10.1002/cssc.200700056

Turpin BJ, Huntzicker JJ (1995) Identification of secondary organic aerosol episodes and quantitation of primary and secondary organic aerosol concentrations during SCAQS. Atmos Environ 29:3527–3544. https://doi.org/10.1016/1352-2310(94)00276-q

U.S. EPA (1989) Risk assessment guidance for superfund. In: Part A: Human Health Evaluation Manual. https://www.epa.gov/risk/risk-assessment-guidance-superfund-rags-part. Accessed 22 December 2019

U.S. EPA (2004) Risk assessment guidance for superfund. In: Part E, Supplemental guidance for dermal risk assessment. https://www.epa.gov/risk/risk-assessment-guidance-superfund-rags-part-e. Accessed 22 December 2019

U.S. EPA (2009) Risk assessment guidance for superfund. In: Part F, Supplemental Guidance for Inhalation Risk Assessment. https://www.epa.gov/risk/risk-assessment-guidance-superfund-rags-part-f. Accessed 22 December 2019

U.S. EPA (2011a) The screening level (RSL) Tables (last updated June 2011). Available on-line at: http://www.epa.gov/region9/superfund/prg/index.html Accessed 15 February 2020

U.S. EPA (2011b) User's guide and background technical document for US EPA region 9's Preliminary remediation goals (PRG) table. http://www.epa.gov/reg3hwmd/risk/human/rb-concentrationtable/usersguide.htm Accessed 15 February 2020

U.S. EPA (2014) Positive Matrix Factorization (PMF) 5.0 Fundamentals and User Guide. Office of Research and Development, Washington, DC. https://www.epa.gov/sites/production/files/2015-02/documents/pmf_5.0_user_guide.pdf Accessed 15 February 2020

Wang AQ (2016) Pollution characteristics of air fine particulate matter ($PM_{2.5}$) in Xuchang. Environ Sci Manag (in Chinese) 41:139–141. https://doi.org/10.3969/j.issn.1673-1212.2016.01.039

Wang Y, Zhuang GS, Sun YL, An ZS (2006) The variation of characteristics and formation mechanisms of aerosols in dust, haze, and clear days in Beijing. Atmos Environ 40:6579–6591. https://doi.org/10.1016/j.atmosenv.2006.05.066

Wang LT, Wei Z, Yang J, Zhang Y, Zhang FF, Su J, Meng CC, Zhang Q (2014) The 2013 severe haze over southern Hebei, China: model evaluation, source apportionment, and policy implications. Atmos Chem Phys 14:3151–3173. https://doi.org/10.5194/acp-14-3151-2014

Wang J, Li X, Jiang N, Zhang W, Zhang R, Tang X (2015) Long term observations of $PM_{2.5}$-associated PAHs: comparisons between normal and episode days. Atmos Environ 104:228–236. https://doi.org/10.1016/j.atmosenv.2015.01.026

Wang F, Guo Z, Lin T, Rose NL (2016) Seasonal variation of carbonaceous pollutants in $PM_{2.5}$ at an urban 'supersite' in Shanghai, China. Chemosphere 146:238–244. https://doi.org/10.1016/j.chemosphere.2015.12.036

Wang LM, Wang XY, Wang MS, Yu GQ, Liu XY, Wang ZF, Pan XL (2020a) Spatial and temporal distribution and potential source of atmospheric pollution in Jiaozuo City. Res Environ Sci (in Chinese) 33(4):820–830. https://doi.org/10.13198/j.issn.1001-6929.2019.04.22

Wang Q, Dong Z, Guo Y, Yu F, Zhan ZY, Zhang RQ (2020b) Characterization of $PM_{2.5}$-bound polycyclic aromatic hydrocarbons at two central China cities: seasonal variation, sources, and health risk assessment. Arch Environ Contam Toxicol 78(1):20–33. https://doi.org/10.1007/s00244-019-00671-4

Widory D (2006) Lead isotopes decipher multiple origins within single PM_{10} samples in the atmosphere of Paris. Isot Environ Health Stud 42:97–105. https://doi.org/10.1080/10256010500502736

Yang Y, Wang Y, Huang W, Hu B, Wen T, Zhao Y (2010) Size distributions and elemental compositions of particulate matter on clear, hazy and foggy days in Beijing, China. Adv Atmos Sci 27:663–675. https://doi.org/10.1007/s00376-009-8197-1

Yang YR, Liu XG, Qu Y, An JL, Jiang R, Zhang YH, Sun YL, Wu ZJ, Zhang F, Xu WQ, Ma QX (2015) Characteristics and formation mechanism of continuous hazes in China: a case study during the autumn of 2014 in the North China Plain. Atmos Chem Phys 15: 8165–8178. https://doi.org/10.5194/acp-15-8165-2015

Yao L, Yang LX, Yuan Q, Yan C, Dong C, Meng CP, Sui X, Yang F, Lu YL, Wang WX (2016) Sources apportionment of $PM_{2.5}$ in a background site in the North China Plain. Sci Total Environ 541:590–598. https://doi.org/10.1016/j.scitotenv.2015.09.123

Zhang YX, Shao M, Zhang YH, Zeng LM, He LY, Zhu B, Wei YJ, Zhu XL (2007) Source profiles of particulate organic matters emitted from cereal straw burnings. J Environ Sci 19:167–175. https://doi.org/10.1016/S1001-0742(07)60027-8

Zhang R, Jing J, Tao J, Hsu SC, Wang G, Cao J, Lee CSL, Zhu L, Chen Z, Zhao Y, Shen Z (2013) Chemical characterization and source apportionment of $PM_{2.5}$ in Beijing: seasonal perspective. Atmos Chem Phys 13:7053–7074. https://doi.org/10.5194/acp-13-7053-2013

Zhang RY, Wang GH, Guo S, Zamora ML, Ying Q, Lin Y, Wang WG, Hu M, Wang Y (2015a) Formation of urban fine particulate matter. Chem Rev 115:3803–3855. https://doi.org/10.1021/acs.chemrev.5b00067

Zhang F, Wang ZW, Cheng HR, Lv XP, Gong W, Wang XM, Zhang G (2015b) Seasonal variations and chemical characteristics of $PM_{2.5}$ in Wuhan, central China. Sci Total Environ 518-519:97–105. https://doi.org/10.1016/j.scitotenv.2015.02.054

Zhao XJ, Zhang XL, Xu XF, Xu J, Meng W, Pu WW (2009) Seasonal and diurnal variations of ambient $PM_{2.5}$ concentration in urban and rural environments in Beijing. Atmos Environ 43:2893–2900. https://doi.org/10.1016/j.atmosenv.2009.03.009

Zhao XJ, Zhao PS, Xu J, Meng W, Pu WW, Dong F, He D, Shi QF (2013) Analysis of a winter regional haze event and its formation mechanism in the North China Plain. Atmos Chem Phys 13:5685–5696. https://doi.org/10.5194/acp-13-5685-2013

Zheng M, Zhang Y, Yan C, Zhu X, Schauer JJ, Zhang Y (2014) Review of $PM_{2.5}$ source apportionment methods in China (in Chinese). Acta Sci Nat Univ Pekin 50:1141–1154. https://doi.org/10.13209/j.0479-8023.2014.068